PORTIONS
OF THIS
DOCUMENT
ARE
ILLEGIBLE

LA-UR-82-1665

CONF-830103--7

Los Alamos National Laboratory is operated by the University of California for the United States Department of Energy under contract W-7405-ENG-36

MASTER

LA-UR--82-1665

DE82 018382

TITLE: POSTTEST ANALYSIS OF SEMISCALE TESTS S-UT-6 AND S-UT-7 USING TRAC PF1

AUTHOR(S): Brent E. Boyack

SUBMITTED TO: Second International Topical Meeting on Nuclear Reactor Thermalhydraulics, January 11-14, 1983, Santa Barbara, California

Los Alamos Los Alamos National Laboratory
Los Alamos, New Mexico 87545

POSTTEST ANALYSIS OF SEMISCALE TESTS S-UT-6 AND S-UT-7 USING TRAC-PF1*

by

B. E. Boyack

Safety Code Development Group
Energy Division
Los Alamos National Laboratory
Los Alamos, NM 87545

ABSTRACT

A posttest study of Semiscale Tests S-UT-6 and S-UT-7 has been completed to assess TRAC-PF1 predictions of pressurized water-reactor (PWR) small-break transients. The comparisons of the TRAC calculations and experimental results show that the correct qualitative influence of upper-head injection (UHI) was predicted. The major phenomenological difference predicted was the mode of core voiding. The data show a slow boiloff from the top of the core resulting in a dryout near the top of the core only. TRAC predicted a more extensive voiding with fluid forced from the bottom of the core by a pressure increase in the upper vessel plenum. The pressure increase was the primary consequence of a failure to predict a complete clearance of the seal in the intact-loop pump-suction upflow leg. Further review of the interphasic drag correlations, entrainment correlations, and critical-flow model is recommended.

---

*Work performed under the auspices of the US Nuclear Regulatory Commission.

I. INTRODUCTION

A paired experiment set conducted in the Semiscale Mod-2A facility at the Idaho National Engineering Laboratory (INEL) has been selected as one element in the Transient Reactor Analysis Code (TRAC)-PF1 assessment program. The tests selected were S-UT-6 and S-UT-7, which simulated a small-break loss-of-coolant accident (LOCA) resulting from a 5% communicative break in the cold leg of a pressurized water reactor (PWR). The test specifications were identical except for upper-head injection (UHI) in Test S-UT-7. TRAC-PF1 (Ref. 1) is the latest version of the TRAC computer code developed for predicting LOCA events in a PWR. While retaining all the essential features of earlier code versions, TRAC-PF1 specifically was developed as a fast-running version for long transients such as small-break LOCAs.

II. SEMISCALE MOD-2A SYSTEM DESCRIPTION

The Semiscale Mod-2A system[2,3] is a scaled integral test facility at INEL used to obtain thermal-hydraulic data for a variety of postulated transients and operating conditions. The Mod-2A system (Fig. 1) is a two-loop PWR primary-coolant-system simulator. The intact loop is scaled to simulate three loops of a large PWR, and the broken loop simulates a single loop in which a break is postulated to occur. Geometric similarity has been maintained between a PWR and Mod-2A, most notably in the design of a full-length (3.66-m) electrically heated core, full-length upper plenum and upper head, component layout, and relative elevations of various components. Major configuration changes between the Mod-2A configuration and the previous Mod-3 configuration resulted from:

1. installation of a new intact-loop steam generator,
2. modification of the broken-loop steam generator,
3. addition of external heaters on the outside surfaces of the coolant piping, and
4. installation of insulation inside the downcomer and lower pressure vessel plenum.

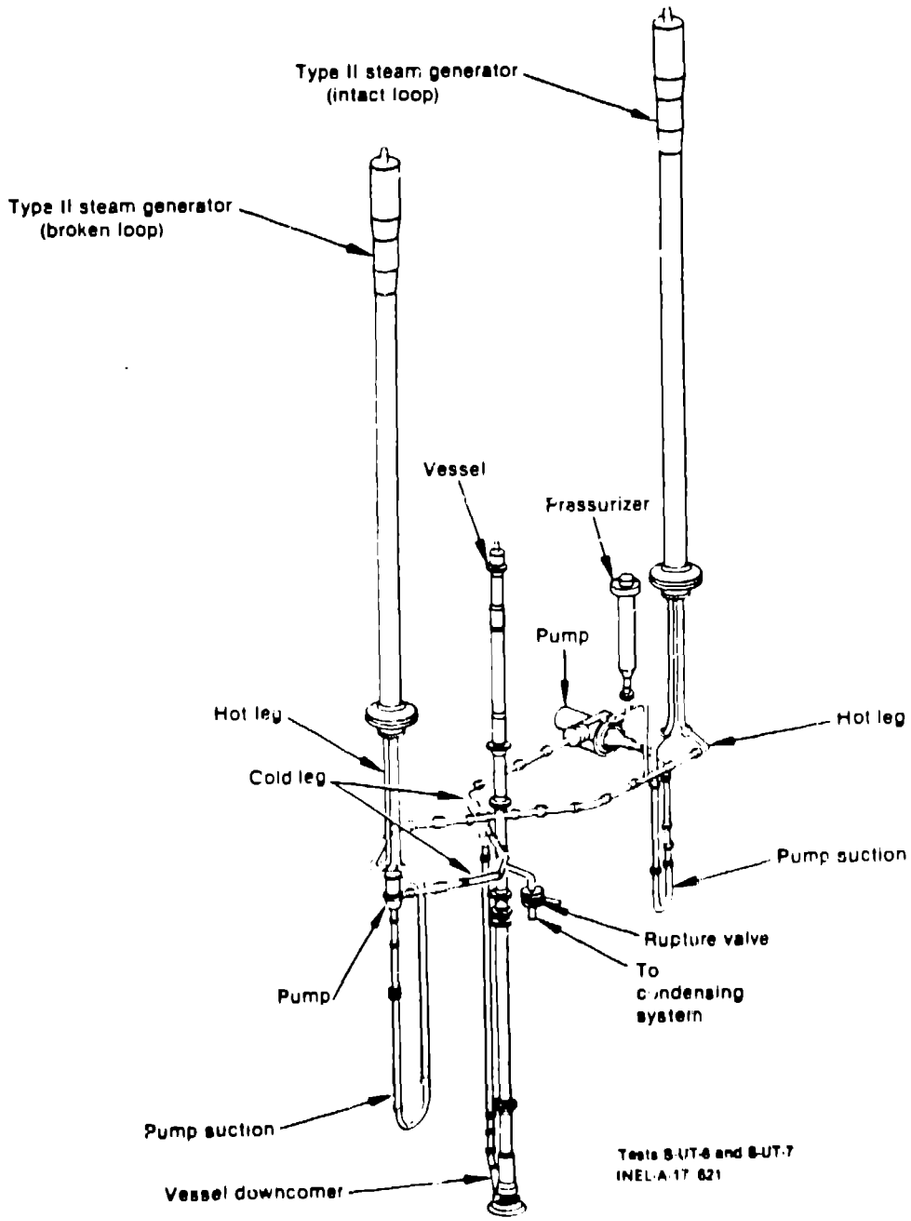

Fig. 1.
Semiscale Mod-2A system isometric (cold-leg-break configuration).

III. TEST DESCRIPTION

Semiscale small-break Tests S-UT-6 and S-UT-7 (Ref. 4) simulated a LOCA resulting from a 5% communicative break in the cold leg of a PWR. The break size for each test was 0.1123 cm^2, which was volumetrically scaled to represent a 15.6-cm-diam pipe break in a PWR. The Mod-2A system for Test S-UT-7 was configured to simulate a PWR with emergency-core-coolant (ECC) injection into the vessel upper head. The upper head accumulator was pressurized to 8.6 MPa and the loop accumulator pressures were set at 2.86 MPa, as is nominally specified for UHI plants. Initial conditions for S-UT-6 were identical to S-UT-7, except UHI was not specified. The remaining initial test conditions were equivalent to or scaled from typical PWR operating conditions. The tests were conducted as specified[5] except that the broken-loop, high- and low-pressure injection pump was mistakenly not operated during Test S-UT-7. The primary objective of the tests was to investigate the distribution of UHI water (and its influence on transient behavior) through comparisons between Semiscale Mod-2A tests S-UT-6 and S-UT-7.

IV. TRAC MODEL

The TRAC input model for the Semiscale Mod-2A facility is shown in Fig. 2a and -b in its cold-leg-break configuration. The input model consisted of 49 one-dimensional components containing a total of 187 computational cells. Table I lists the components. The input model corresponded to the Semiscale Mod-2A hardware configuration with the following exceptions.

1. The pressure-suppression system was modeled indirectly. A BREAK component was introduced and the pressure and temperature at the break were specified as boundary conditions.

2. The secondary feedwater systems, both main and auxiliary, were represented by FILL components 7 and 26 for the intact and broken loops, respectively.

3. The high-pressure injection system (HPIS) was represented by FILL components 13 and 43 for the intact and broken loops, respectively.

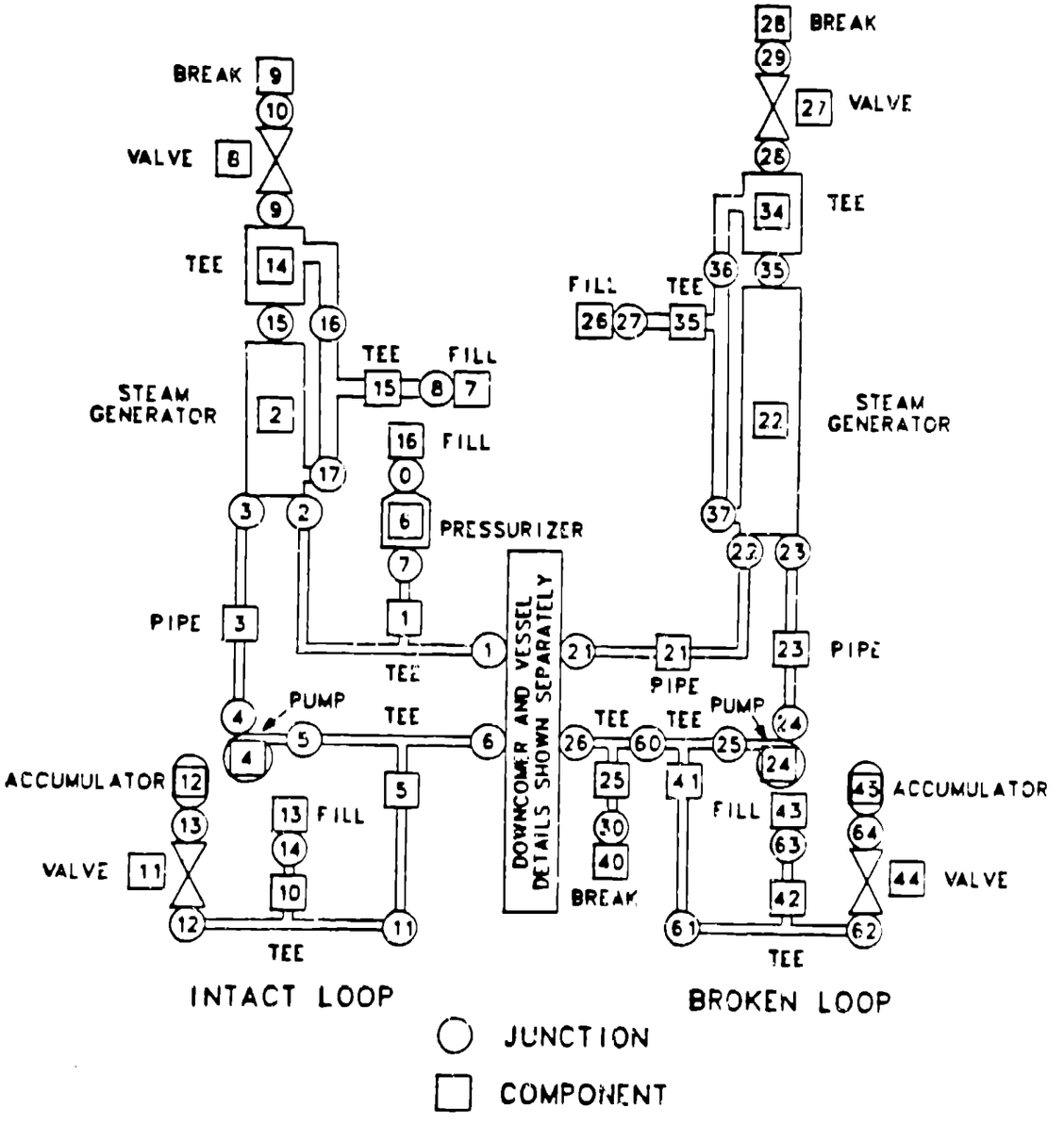

Fig. 2a.
TRAC input model for the Semiscale Mod-2A facility.

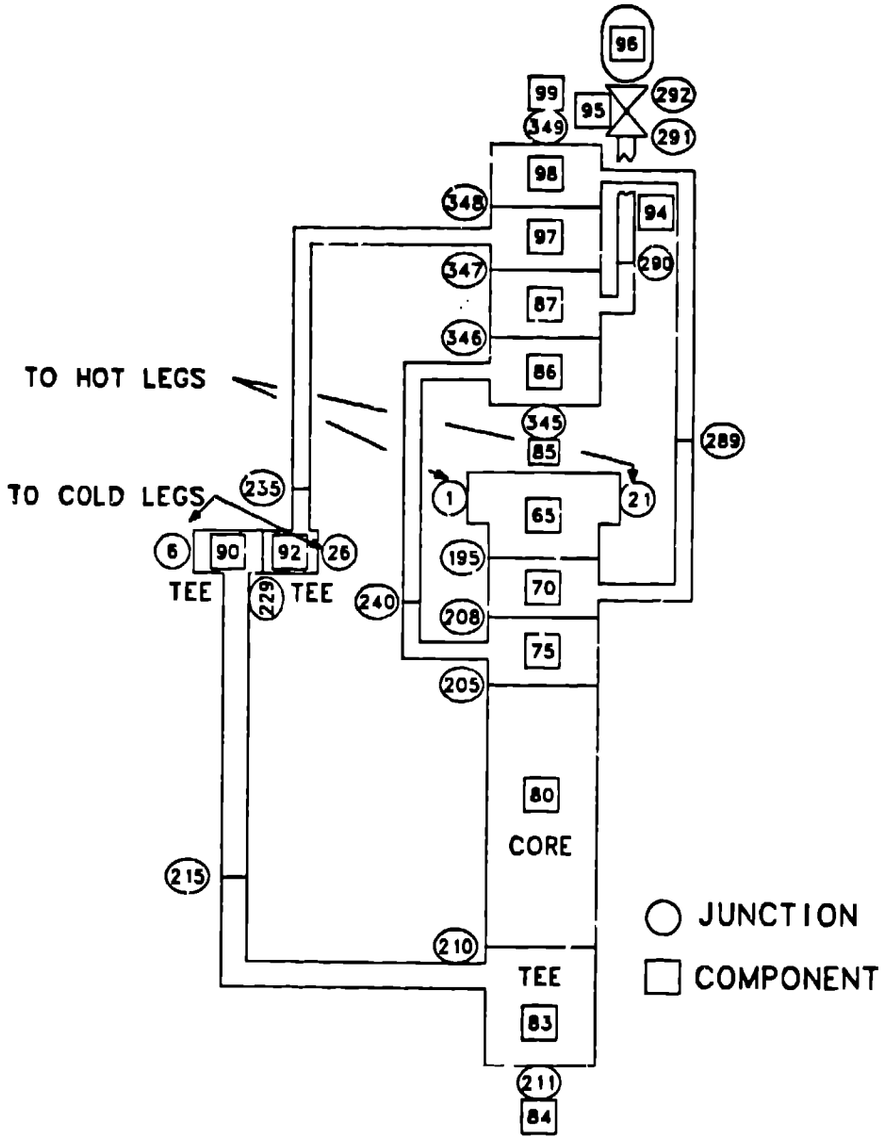

Fig. 2b.
TRAC downcomer and vessel noding for the Semiscale Mod-2A Facility.

TABLE I

TRAC MODEL COMPONENTS

Component Number[a]	Component Type	Description	Number of Fluid Cells (Primary Side Secondary Side)[b]
1	TEE	Intact-loop hot leg	4, 3
2	STGEN	Intact-loop steam generator	10, 5
3	PIPE	Intact-loop pump suction	10
4	PUMP	Intact-loop pump	2
5	TEE	Intact-loop cold leg	4, 1
6	PRIZER	Intact-loop pressurizer	5
7	FILL	Intact-loop steam-generator feedwater	1
8	VALVE	Intact-loop steam line	2
9	BREAK	Intact-loop steam-generator-secondary pressure set point	1
10	TEE	Intact-loop ECC line	2, 1
11	VALVE	Intact-loop accumulator valve	2
12	ACCUM	Intact-loop accumulator	4
13	FILL	Intact-loop High pressure injection system	1
14	TEE	Intact-loop steam-generator-secondary steam dome	2, 1
15	TEE	Intact-loop steam-generator-secondary downcomer	5, 1
16	FILL	Pressurizer inlet	1
21	PIPE	Broken-loop hot leg	3
22	STGEN	Broken-loop steam generator	12, 6
23	PIPE	Broken-loop pump suction	7
24	PUMP	Broken-loop pump	2
25	TEE	Broken-loop cold leg	3, 2
26	FILL	Broken-loop steam-generator feedwater	1
27	VALVE	Broken-loop steam line	2
28	BREAK	Broken-loop steam-generator-secondary pressure set point	1
34	TEE	Broken-loop steam-generator-secondary steam dome	2, 1
35	TEE	Broken-loop steam-generator-secondary downcomer	6, 1
40	FILL, BREAK	Fill for steady-state run, break for transient run	1
41	TEE	Broken-loop cold leg	3, 1
42	TEE	Broken-loop ECC line	2, 1
43	FILL	Broken-loop HPIS	1
44	VALVE	Broken-loop accumulator valve	2
45	ACCUM	Broken-loop accumulator	4

TABLE I (continued)

Component Number[a]	Component Type	Description	Number of Fluid Cells (Primary Side Secondary Side)[b]
65	TEE	Upper section of upper plenum	1, 1
70	PIPE	Middle section of upper plenum	1
75	TEE	Lower section of upper plenum and guide and core support tubes	1, 1
80	CORE	Core	9
83	TEE	Lower plenum	3, 2
84	FILL	Bottom lower plenum	1
85	FILL	Bottom upper head	1
86	TEE	Lower section of upper head	1, 2
87	TEE	Lower mid section of upper head	1, 2
90	TEE	Intact-loop side downcomer inlet and downcomer	2, 10
92	TEE	Broken-loop side downcomer inlet and upper-head bypass	2, 1
94	PIPE	Upper head injection tube	2
95	VALVE	Upper head injection valve	2
96	ACCUM	Upper head injection accumulated	2
97	TEE	Mid upper section of upper head	1, 2
98	TEE	Upper section of upper head	2, 1
99	FILL	Top upper head	1

[a]The total number of components is 49.

[b]The total number of cells is 187.

The TRAC-PF1 choked-flow model was used to calculate the break flow. The break orifice had a rounded entrance with a length-to-diameter ratio of 3.35 (length, 12.65 mm; diameter, 3.78 mm). Thus, the secondary side of break TEE 25 for this test was modeled using two cells with the second cell representing the break orifice.

Power tables were defined for the pipe and TEE components representing the primary-loop piping to simulate the external heaters used during the test. A new pipe material was defined for the downcomer tube (TEE 90 secondary) and the vessel lower plenum (PIPE 83) to simulate the thermal conductivity of a composite steel wall clad with honeycomb insulation. Primary-system heat losses to the environment were set to the values reported in Ref. 6. The intact- and broken-loop steam generators were modified to reflect the geometry and heat-transfer characteristics of the Type-II steam generator installed in the Mod-2A facility.

V. RESULTS

The following sections present and discuss the results obtained during posttest predictions of Semiscale Mod-2A Tests S-UT-6 and S-UT-7. Detailed results are presented only for Test S-UT-7, as the influence of UHI was small and the results for the two tests were similar. For Test S-UT-7, a discussion of the general system behavior is presented, followed by more detailed descriptions of factors that influenced the calculated system response. In the figures presented, TRAC calculated results are labeled as either BASE (base-case calculation) or PARAMETRIC (parametric calculation). Test data are labeled TEST. The results section is concluded with a summary description of Test S-UT-6 results, including a discussion of similarities and differences relative to Test S-UT-7.

A. General System Behavior

The initial conditions and specified test parameters for Test S-UT-7 are presented in Table II. The calculated loop flow rates, which were less than measured, were specified by the pump speeds with the objective of matching the measured hot- and cold-leg fluid temperatures. In general, the steady state calculated by TRAC matched the test conditions very well.

TABLE II

TEST S-UT-7 INITIAL CONDITIONS

Parameter	Actual	Calculated
Core Power (MW)[a]	1.994	1.994[b]
Pressurizer pressure (MPa)	15.5	15.5[b]
Pressurizer liquid mass (kg)	10.4	10.2
Intact-loop mass flow (kg/s)	6.77	6.4
Intact-loop cold-leg temperature (K)	558.	557.2
Intact-loop hot-leg temperature (K)	599.	598.2
Broken-loop mass flow (kg/s)	2.1	2.1
Broken-loop cold-leg temperature (K)	559.	558.7
Broken-loop hot-leg temperature (K)	598.	598.2
Intact-loop pump speed (rad/s)	198.3	199.5[b]
Broken-loop pump speed (rad/s)	974.3	1280.[b]
Intact-loop steam-generator-secondary pressure (MPa)	5.7	5.5
Intact-loop steam-generator-secondary feedwater temperature (K)	502.	502.[b]
Broken-loop steam-generator-secondary pressure (MPa)	5.9	5.4
Broken-loop steam-generator-secondary feedwater temperature (K)	497.	497.[b]

[a]Flat radial profile.

[b]Specified as input parameter.

Table III presents the calculated event times for Test S-UT-7. The timing of events during subcooled blowdown was predicted quite well. Events during the two-phase blowdown were not calculated as well. The clearance of the intact-loop pump-suction seal was predicted to occur approximately 40 s later than measured. This delay occurred because the calculated break flow during saturated blowdown and before clearance of the loop seals was less than measured. Complete clearance of liquid in the intact-loop pump-suction piping was not predicted during the calculation. Predicted core liquid levels were less than measured following clearance of the intact-loop seal. This resulted in a more extensive dryout of the core than measured. It appears that the underpredicted core liquid level and associated dryout were directly related to the failure to predict total clearance of liquid in the intact-loop pump-suction upflow leg. The remaining liquid may have produced sufficient sealing to increase the pressure back through the intact loop to the upper

TABLE III

TEST S-UT-7 EVENTS

Event	Time (s)		
	Actual	Base Case	Parametric Case
Blowdown initiated	0.	0.	0.
Pressure trip	8.6	9.2	8.8
Intact- and broken-loop main steam valves begin closing	10.8	11.5	11.1
Core power decay initiated	12.4	13.0	12.4
Intact- and broken-loop pump coastdown initiated	14.2	14.8	14.3
Upper head injection begins	21.	26.8	25.5
Intact-and broken-loop main feedwater valves begin to close	34.	34.5	34.3
Broken-loop pump stops	77.	77.7	77.5
Intact-loop pump stops	136.	135.4	135.2
Intact-loop pump suction blows out	220.	261.	180.
Upper head accumulator injection ends	296.	~300.	~240.
Intact-loop pump suction cleared of liquid	650.	no	no
Intact- and broken-loop accumulator injection begins	738.	659.5	770.8
Broken-loop accumulator injection ends	1810.	1950.	NA
Intact-loop accumulator injection ends	3730.	3725.[a]	NA

[a]Six-cm water remained.

vessel plenum. The increased pressure induced a flow reversal in the core that led to a dryout at the center of the core. In contrast, the dryout occurring in the test resulted from the slow boil-off of liquid until the top 60 cm of the core uncovered.

B. Break Flows

The calculated base-case and measured break flows are shown in Fig. 3. The test data show a sharp drop in break flow beginning at approximately 220 s. The reduced flow was attributed to the cleared seal in the intact-loop pump-suction pipe and the uncovered break orifice.[7] The latter phenomenon is

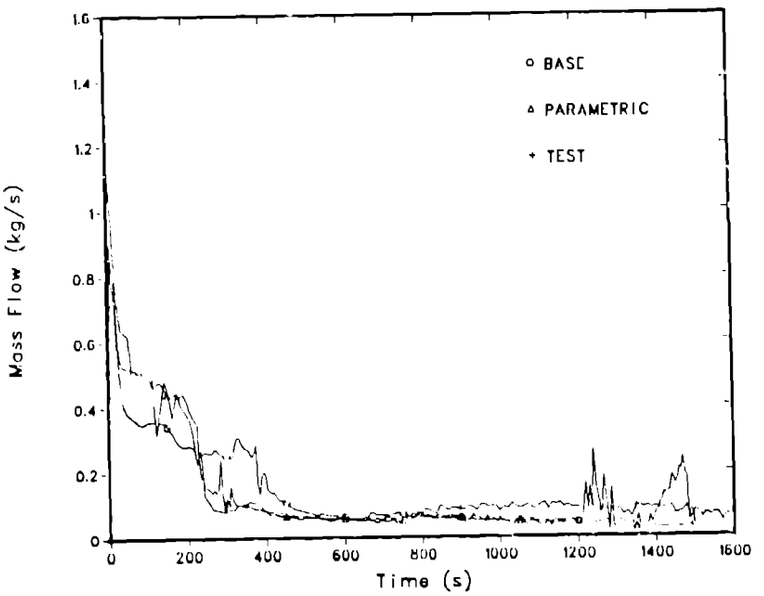

Fig. 3.
Break flow for Test S-UT-7.

clearly two-dimensional, while the models of system piping are all one-dimensional. The break flows calculated by the TRAC-PF1 critical-flow model during the subcooled blowdown (from rupture until approximately 40 s) and during saturated blowdown of a two-phase fluid were too low. Because the break flows were underpredicted, the clearance of the loop seal and uncovery of the break orifice were delayed. At approximately 220 s the calculated break flow exceeded that measured because the latter had sharply decreased with uncovery of the break orifice, resulting in the exhaust of steam only through the break.

The sharp increase in calculated break flow at approximately 280 s was induced by a flow reversal in the core that pushed fluid out the bottom of the core, through the downcomer, and out the break. This phenomenon appears to be associated with the failure to predict a complete clearing of liquid in the intact-loop pump-suction piping as will be discussed later. A second sharp increase in calculated break flow occurred at ~1400 s. At this time the system pressure began to decay rapidly, followed by a partial recovery ~100 s later. During the pressure decay the accumulators injected a large volume of liquid,

some of which flowed out the break. We have not been able to identify the cause for the sharp pressure decay.

The measured break flow increased at ~700 s but the magnitude of this measurement appears in error. Integration of the measured instantaneous break flow to 4500 s yielded a total break flow of ~450 kg, while the catch tank measurement of break flow was ~275 kg. At 4500 s the calculated integrated break flow was ~290 kg. The calculated base-case and measured integrated break flows are compared in Fig. 4. The knee in the measured integrated mass flow occurred when the break orifice uncovered and passed steam only. At 220 s the underprediction of integrated break flow was at a maximum of ~25 kg. In a later section, results of a parametric study using multipliers to adjust the predicted break flow will be discussed.

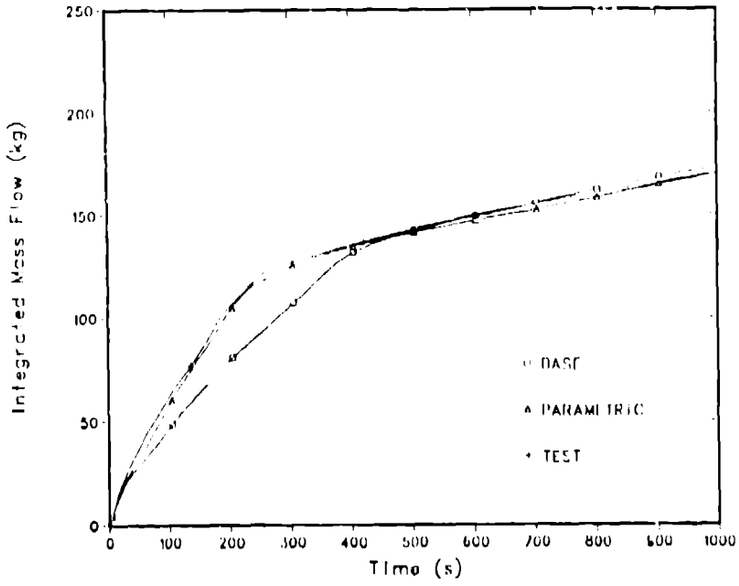

Fig. 4.
Integrated break flow for Test S-UT-7.

C. System Pressure

The calculated base-case and measured system pressure responses for Test S-UT-7 are compared in Fig. 5. The calculated pressure was overpredicted until 450 s. This corresponded closely with the underprediction of integrated break flow shown in Fig. 4. The increased rate of system depressurization beginning at approximately 360 s was due to a steep drop in density upstream of the break that occurred following the initial clearance of the intact-loop pump-suction seal and by voiding in the core that reduced heat transfer to the primary-cooling system fluid.

D. Loop Hydraulic Response

Deviations from the measured hydraulic performance in the loops can be understood by reviewing two features of the calculated performance that differ from those measured. The first factor has been discussed already. The critical-flow model underpredicted the break flow during the first 220 s of the transient. Thus, liquid was retained in the loops and clearance of the loop

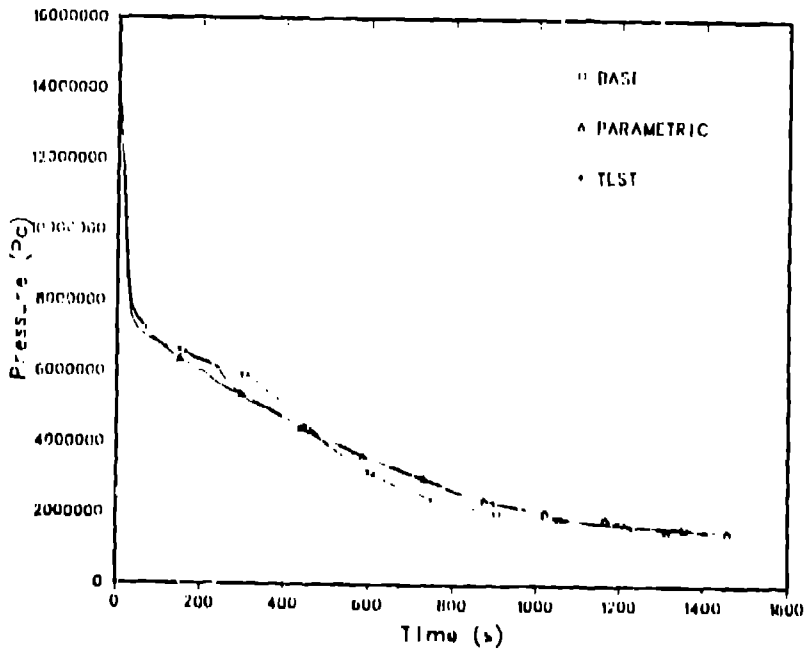

Fig. 5.
System pressure response for Test S-UT-7.

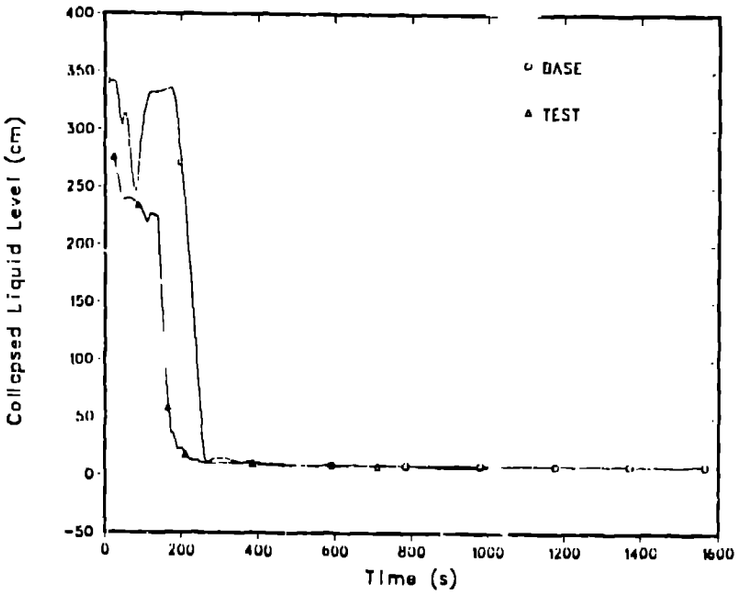

Fig. 6.
Collapsed liquid level in intact-loop pump-suction downflow leg for Test S-UT-7.

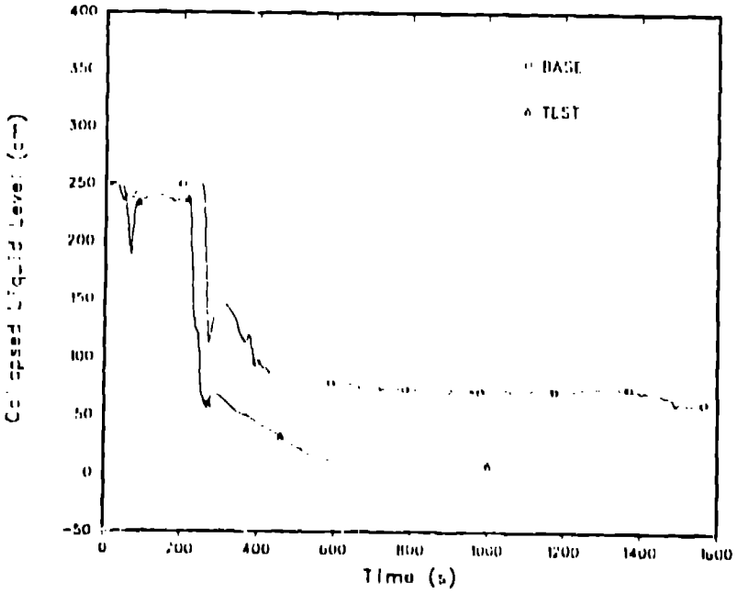

Fig. 7.
Collapsed liquid level in intact-loop pump-suction upflow leg for Test S-UT-7.

seals was delayed. The collapsed liquid levels in the intact-loop pump-suction downflow leg and upflow leg are shown in Figs. 6 and 7. The delayed clearance of the intact-loop pump-suction downflow leg is clearly shown in Fig. 6. Figure 7 displays the second factor thought to result in the calculated loop hydraulic response deviating from that measured. Again, the initial clearing of the loop seal is shown. However, the remaining liquid in the upflow leg failed to clear as observed in the test, which resulted in reduced mass flow through the intact loop. One possible reason for predicting the retention of liquid in the upflow leg may be the underprediction of interfacial shear and entrainment that lifts the remaining liquid out of the leg. Figures 8 and 9 show the calculated and measured mass flows in the hot and cold legs of the intact loop, respectively. Following establishment of the loop seal during the test, flow through the intact loop stopped. Flow was re-established following clearance of the loop seal. Because liquid remained in the upflow leg following the initial clearance of the loop seal, no such re-establishment of flow was calculated.

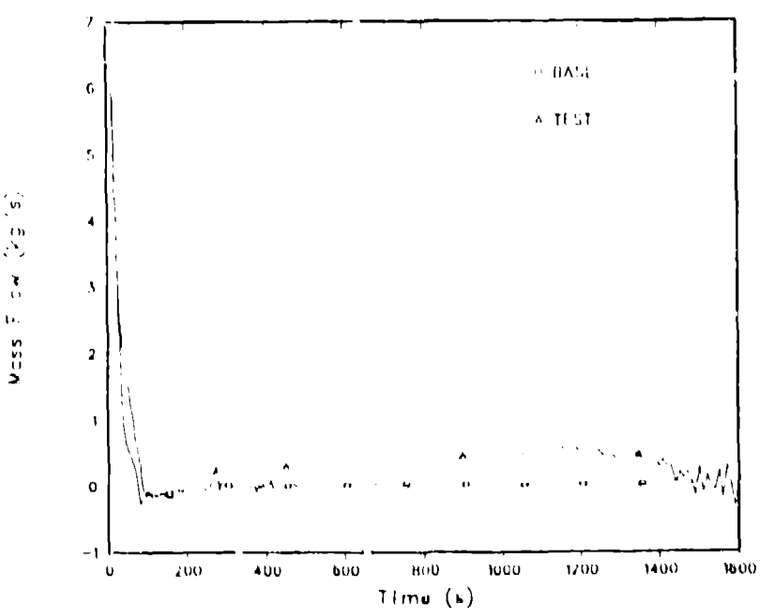

Fig. 8.
Intact-loop hot-leg mass flow for Test S-UT-7.

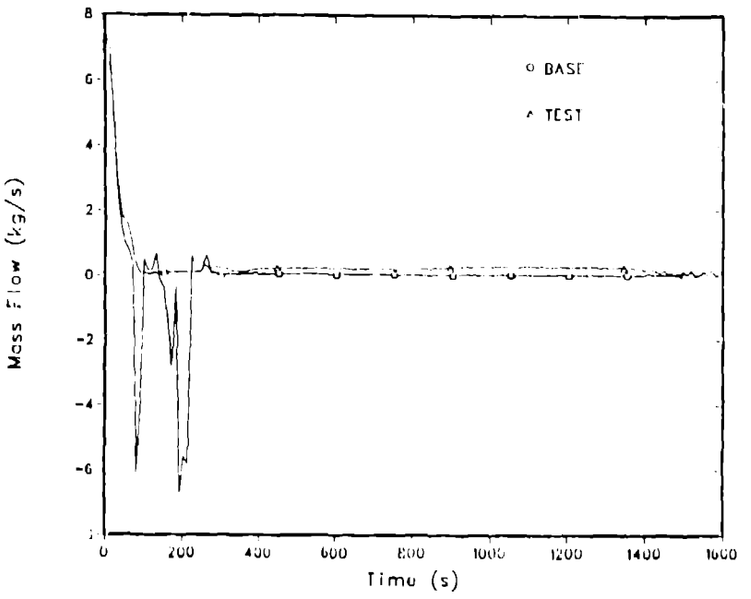

Fig. 9.
Intact-loop cold-leg mass flow for Test S-UT-7.

The collapsed liquid levels in the broken-loop pump-suction downflow and upflow legs are shown in Figs. 10 and 11. In the downflow leg the calculated clearance of the loop seal was delayed. The data also show a slight refilling of the downflow leg between 400 and 1400 s that was not calculated. In the upflow leg, a more rapid initial clearance of the loop seal was calculated. Liquid remained in the upflow leg during the test and a similar result was predicted by TRAC-PF1. Figure 12 shows the calculated and measured mass flows in the pump-suction leg of the broken loop. The mass flow trends in the broken-loop pump suction were predicted well.

E. Core Behavior

The calculated and measured collapsed core liquid levels shown in Fig. 13 exhibit significant differences. The data showed a decrease in the liquid level until 220 s, after which clearance of the loop seal permitted liquid to re-enter the core. By 400 s a slow boiloff began and continued to 800 s. The turnaround resulted from ECC injections from the intact- and broken-loop accumulators. Calculated performance was similar until approximately 300 s.

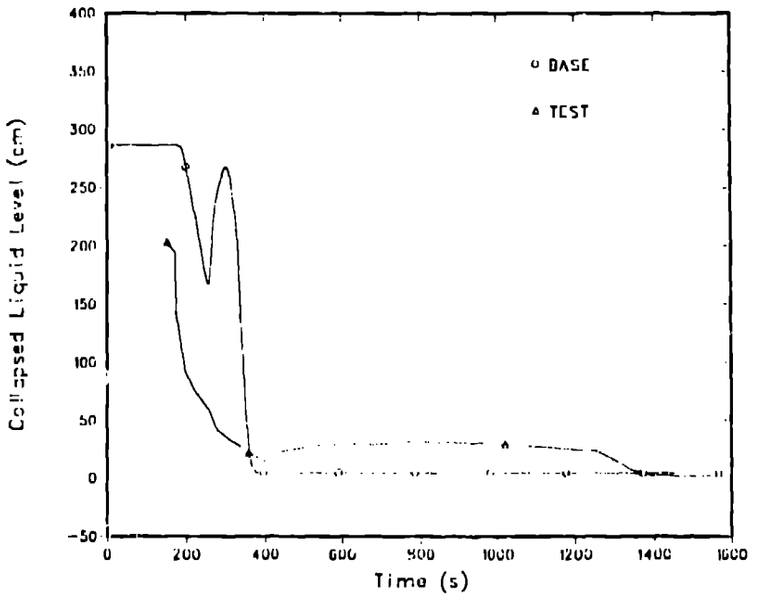

Fig. 10.
Collapsed liquid level in the broken-loop pump-suction downflow leg for Test S-UT-7.

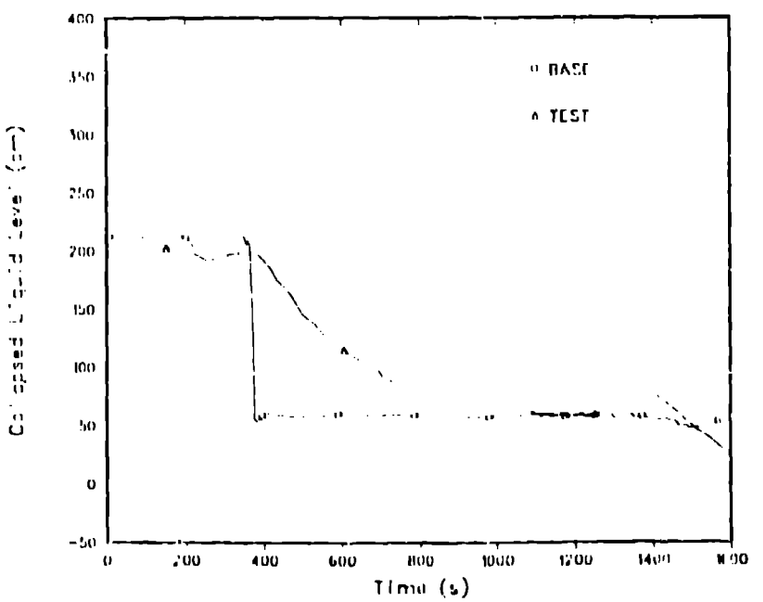

Fig. 11.
Collapsed liquid level in the broken-loop pump-suction upflow leg for Test S-UT-7.

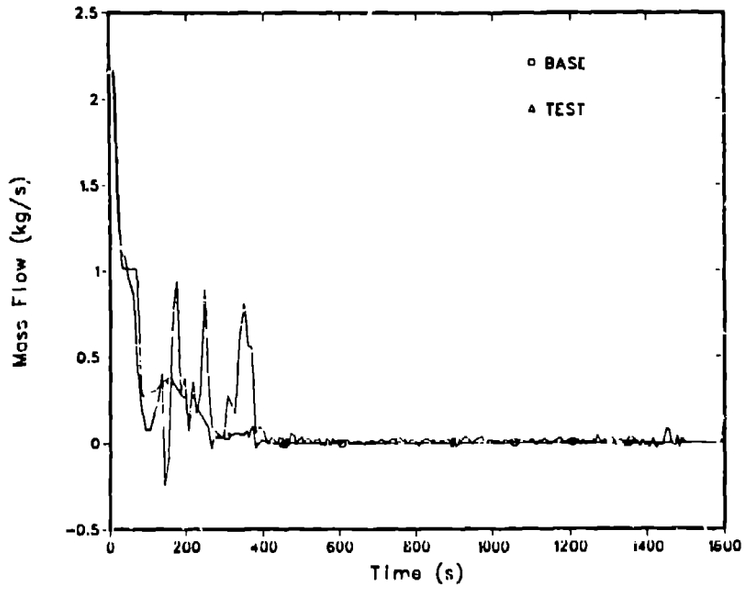

Fig. 12.
Broken-loop pump-suction mass flow for Test S-UT-7.

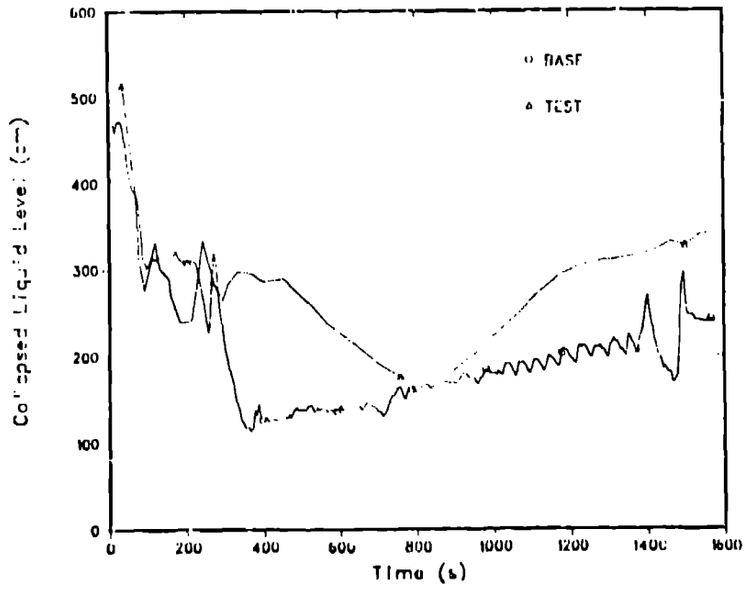

Fig. 13.
Collapsed core liquid levels for Test S-UT-7.

However, just before 300 s a flow reversal in the core was calculated that was a precurser to a mid-core dryout between 325-350 s. Results of the core flow reversal are seen as a sharp decrease in the collapsed liquid level beginning at approximately 300 s. The core coolant inventory decreased approximately 1.5 kg during the flow reversal.

Figures 14-16 compare the calculated and measured fluid densities in the core at levels 13, 183, and 158 cm above the bottom of the heated core. At the 13-cm level, a brief dryout was calculated but its duration was short and no cladding heatup was predicted (Fig. 17). The calculated fluid density at the bottom of the core was generally higher than measured. This suggests that the predicted vapor fractions near the bottom of the core were low. As in the intact-loop pump-suction upflow leg, this result suggests that the interphasic drag or the entrainment rate may be underpredicted. As shown in Fig. 15, a dryout was predicted but not measured at the 182-cm level. This dryout resulted in a large cladding temperature rise as shown in Fig. 18 (at the 195-cm level). At the upper end of the core, the hydraulics were affected

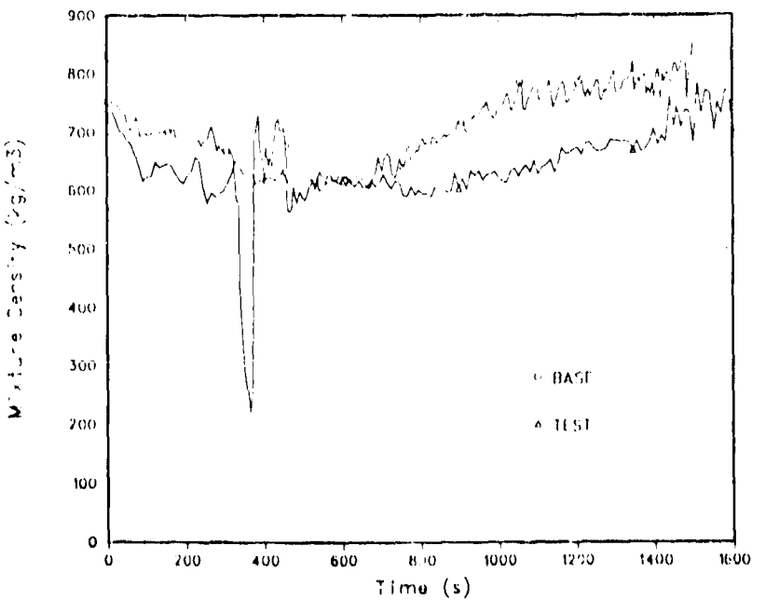

Fig. 14.
Core density at 13-cm level for Test S-UT-7.

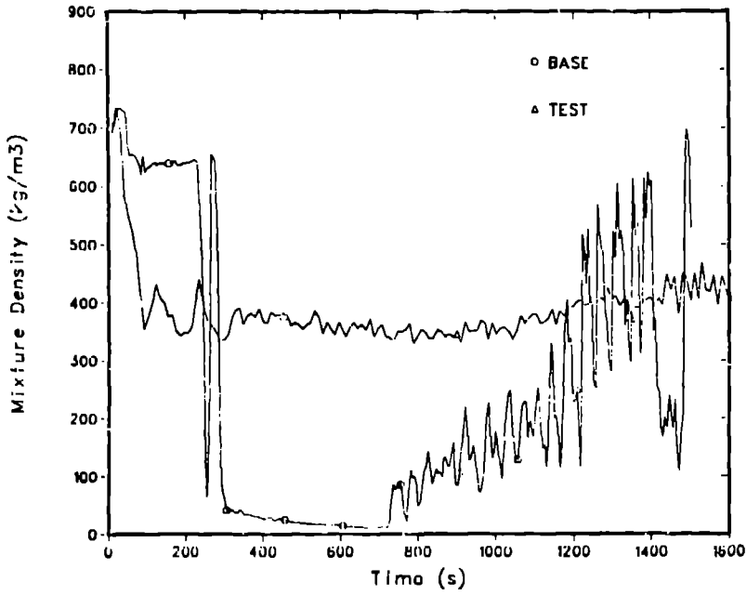

Fig. 15.
Core density at 183-cm level for Test S-UT-7.

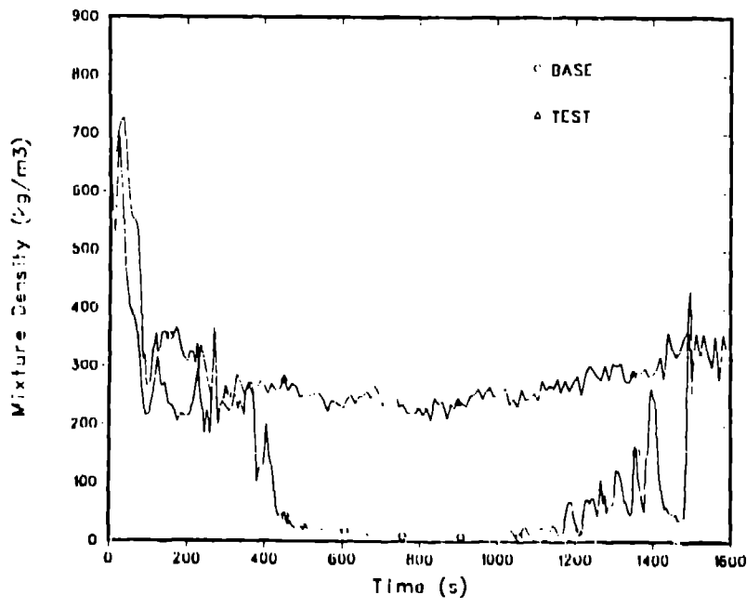

Fig. 16.
Core density at 253-cm level for Test S-UT-7.

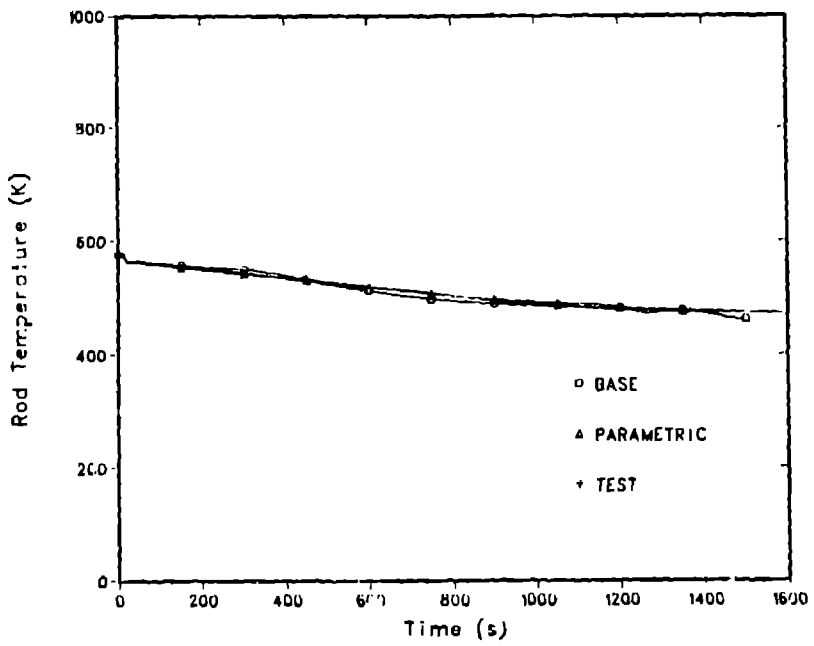

Fig. 17.
Cladding temperature at 13-cm level for Test S-UT-7.

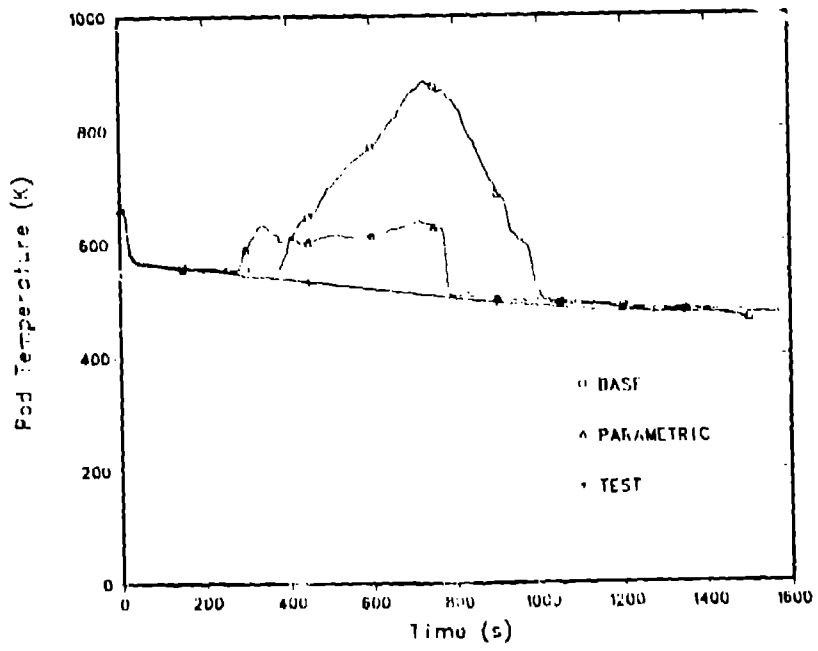

Fig. 18.
Cladding temperature at the 195-cm level for Test S-UT-7.

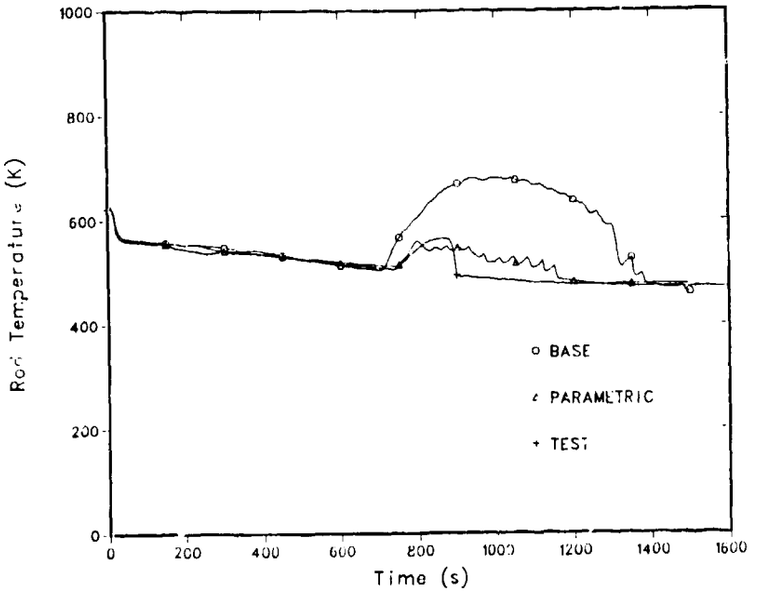

Fig. 19.
Cladding temperature at 321-cm level for Test S-UT-7.

strongly by the UHI phenomenon. Figure 19 shows the cladding temperatures near the top of the heated core (321 cm).

F. Upper Head Fluid Behavior

The behavior predicted in the upper head was similar qualitatively to the test behavior but differed in several details. The initial flows for the bypass, guide, and core support tubes were 0.307 ℓ/s, 0.223 ℓ/s, and 0.084 ℓ/s compared to measured values of 0.33 ℓ/s, 0.242 ℓ/s, and 0.088 ℓ/s, respectively. Transient flows in the upper vessel bypass tube were well predicted both for magnitude and time of flow reversal. The summed result of the various upper-head inflows and outflows is shown in Fig. 20, which displays the collapsed liquid level in the upper head. TRAC predicted an early initial drain of the upper head that was caused by support tube flow exceeding the measured flow by ~50%. Only a slight refill was calculated, whereas the upper head refilled during the final surge of accumulator discharge before 300 s. The deviations from measured performance in the upper head did not significantly influence the overall system performance.

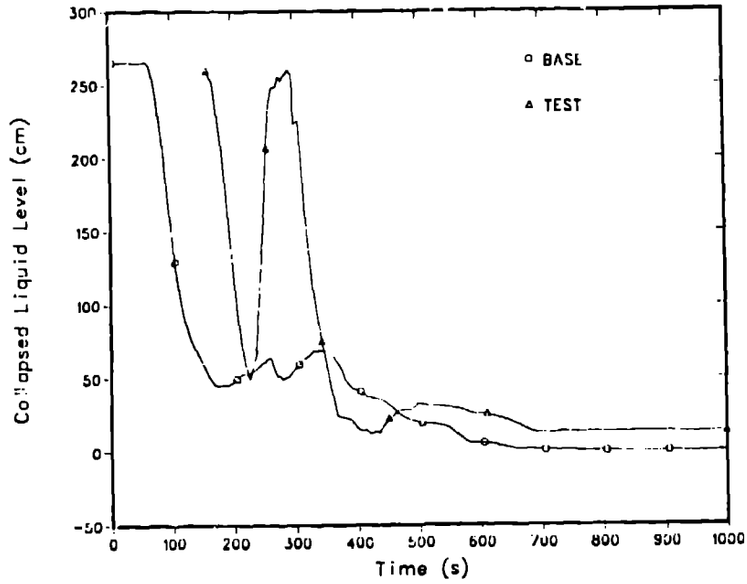

Fig. 20.
Collapsed liquid level in the upper head for Test S-UT-7.

G. Parametric Study

A parametric study was conducted to determine the importance of predicting the break flow closely. The conceptual approach of the study was to specify the measured break flow as a boundary condition. In practice, however, the break flow for Test S-UT-7 could not be specified easily without encountering computational difficulties. Thus, a compromise approach was selected in which the break flow over various intervals was adjusted by specifying multipliers on the TRAC-PF1 critical-flow model. Although not exact, the resultant break flow compared closely with the measured break flow as shown in Fig. 3. Figure 4, which presents the resultant integrated break flow, shows that the specified break flow was a fairly good approximation to the test.

Initial conditions for the parametric study were identical to those for the base case (Table II). The calculated events for the parametric study are presented in Table III.

The comparison between the calculated and measured system pressure response was improved as shown in Fig. 5. The improved system pressure calculation demonstrated the close relationship between the correct calculation of break flow and global characteristics such as system pressure. Deviations from the measured cladding temperature response also were reduced in the parametric study. The calculated and measured cladding temperatures at three core levels are presented in Figs. 17-19. Comparison with the base case shows that the overprediction of cladding temperature was reduced, as well as the duration of the dryout. At the top of the core the prediction was excellent. Prediction of the initial clearance time of the intact-loop pump-suction downflow leg was improved, but the upflow leg seal still failed to clear.

H. Test S-UT-6

Reference 7 reports that the overall effect of UHI on system behavior early in the transient was minimal relative to the response observed in Test S-UT-6. However, the UHI liquid maintained a minimum core-collapsed liquid level ~0.5 m higher than in Test S-UT-6, which improved the margin against severe core heatup.

A comparison of the calculated results for S-UT-7 and S-UT-6 shows the same qualitative trends. For example, the UHI liquid maintained a minimum core-collapsed liquid level ~0.1 m higher than calculated for Test S-UT-6. This provided an additional margin against core heatup. At the 321-cm level the calculated maximum cladding temperature for Test S-UT-7 was ~60 K lower than for Test S-UT-6. Reference 7 reports that typical peak cladding temperatures were ~100 K lower for Test S-UT-7.

The Test S-UT-6 calculation was similar to the Test S-UT-7 base-case calculation in most respects. As with Test S-UT-7, the break flow was underpredicted before the intact-loop loop seal cleared in the test. The predicted voiding characteristics for Test S-UT-6 were very similar to those predicted for Test S-UT-7 with maximum temperatures for the non-UHI test slightly higher. The depletion of core liquid inventory again was caused by failure of the intact-loop pump-suction upflow leg to clear.

V. Timing Data

A complete transient was calculated for Test S-UT-7 only. The CDC-7600 central-processor-unit (CPU) time required for the 4500-s transient was 18061 s. Thus, the ratio of CPU to real time for the transient was 4.01.

VI. CONCLUSIONS

TRAC-PF1 generally predicted well Test S-UT-6 and S-UT-7 transients. The correct qualitative influence of UHI was predicted, although differences were observed between the magnitudes of predicted and measured values of core liquid inventories and cladding temperature responses.

This assessment has identified two features of the code that should be studied further. First, the interphasic drag and entrainment correlations should be reviewed to determine why complete clearance of the intact-loop pump-suction upflow leg was not predicted and why the core liquid inventory (as inferred from density comparisons) appeared to collect at the bottom of the core. Second, the critical-flow model should be re-examined to determine why the subcooled and two-phase saturated blowdown rates were underpredicted. We believe that improving TRAC-PF1 predictions in these two areas will lead to improved predictions of Semiscale small-break transients.

REFERENCES

1. J. H. Mahaffy, D. R. Liles, and T. F. Bott, "TRAC Methods and Models," Proceedings of the American Nuclear Society Specialists Conference on Small Break Loss-of-Coolant Accident Analyses in LWRs, Monterey, California (August 25-27, 1981), Electric Power Research Institute report WS-81-201 (1981).

2. M. L. Patton, "Semiscale MOD-3 Test Program and System Description," NUREG/CR-0239, TREE-NUREG-1212 (July 1978).

3. "Addendum 7, Mod-2A Phase I Addendum to Mod-3 System Description, EG&G Idaho, Inc." (December 1980).

4. R. A. Larson and L. B. Clegg, "Experiment Data Report for Semiscale Mod-2A Small Break Test Series (Tests S-UT-6 and S-UT-7)," EG&G Idaho, Inc. report NUREG/CR-2355 (November 1981).

5. R. G. Hansen, "Experiment Operating Specification for Semiscale Mod-2A 5% Break Experiments S-UT-6 and S-UT-7," EG&G Idaho, Inc. report EGG-SEMI-5421 (April 1981).

6. G. G. Loomis, "Summary Report Semiscale Mod-2A Heat Loss Characterization Test Series," EG&G Idaho, Inc. report EGG-SEMI-5448 (May 1981).

7. R. G. Hansen, D. J. Shimeck, and J. L. Steiner, "Quick Look Report for Semiscale Mod-2A Test S-UT-7," EG&G Idaho, Inc. report EGG-SEMI-5442 (May 1981).